



# Stiffness enhancement analysis of ultrasonic-assisted milling titanium alloy curved thin-walled parts

Jinglin Tong<sup>1</sup> · Penghui Zai<sup>1</sup> · Peng Chen<sup>1</sup> · Ziqiang Liu<sup>1</sup> · Zhiming Zhang<sup>1</sup>

Received: 5 December 2020 / Accepted: 13 July 2021 / Published online: 28 July 2021  
© The Author(s), under exclusive licence to Springer-Verlag London Ltd., part of Springer Nature 2021

## Abstract

Machining of titanium alloy curved thin-walled parts, one of the challenges in aerospace engineering, has attracted much attention. In this article, longitudinal-torsional composite ultrasonic-assisted milling (LTCUVM) was applied to the thin-walled parts, and the stiffness characteristics were studied. Firstly, the cutting edge trajectory of LTCUVM was discussed. Then, the dynamic equation of the thin-walled parts was established, and the stiffness characteristics were theoretically analyzed. Finally, the influences of curvature and machining parameters on the stiffness of the thin-walled parts were studied through experiments. The experimental results showed that the stiffness in LTCUVM was evidently higher than that in CM. With the increase of curvature, the stiffness enhancement multiples of LTCUVM increased first and then decreased. In addition, larger ultrasonic amplitude, smaller feed rate, radial cutting depth, and spindle speed could achieve better stiffness enhancement effect, and the advantages of LTCUVM could be brought into full play. The findings of this research provide an important reference for machining titanium alloy curved thin-walled parts.

**Keywords** Longitudinal-torsional composite ultrasonic-assisted milling · Titanium alloy · Curved thin-walled parts · Stiffness enhancement analysis

## Nomenclature

$v_f$	Feed speed of milling cutter (mm/s)	$\varnothing$	Angle of tool rotation (rad)
$r$	Radius of milling cutter (mm)	$M$	Mass matrix of thin-walled parts (kg)
$n$	Spindle speed (r/min)	$Y$	Deformation matrix in the thickness direction of thin-walled parts (mm)
$f$	Ultrasonic vibration frequency (Hz)	$C$	Damping matrix of thin-walled parts (N · s/mm)
$A$	Amplitude of ultrasonic longitudinal vibration (mm)	$K$	Stiffness matrix of thin-walled parts (N/mm)
$B$	Amplitude of ultrasonic torsional vibration (mm)	$T$	The ultrasonic vibration period of milling cutter (s)
$\theta_1$	Initial phase of ultrasonic longitudinal vibration (rad)	$k_y$	The structural stiffness of thin-walled parts (N/mm)
$\theta_2$	Initial phase of ultrasonic torsional vibration (rad)	$\omega_n$	The natural circular frequency of thin-walled parts (rad)
$F_0$	Amplitude of the contact force (N)	$\tau$	The damping ratio of thin-walled parts
$\omega$	Circular frequency of ultrasonic vibration (rad/s)	$\varphi$	The phase angle of contact force and displacement (rad)
$t_l$	Effective cutting time in one ultrasonic vibration cycle (s)	$k_{ye}$	The stiffness of thin-walled parts (N/mm)
		$f$	First-order natural frequency of thin-walled parts (Hz)

✉ Jinglin Tong  
tongjinglin@hpu.edu.cn

✉ Penghui Zai  
1059696976@qq.com

<sup>1</sup> School of Mechanical and Power Engineering, Henan Polytechnic University, Jiaozuo 45400, Henan, China

## 1 Introduction

Titanium alloy materials are widely used in aerospace, petrochemical, medical equipment, and other fields because of their high specific strength, high-temperature resistance, good corrosion resistance, and low density [1, 2]. In the field of aerospace, more and more parts on aerospace vehicles adopt

integral thin-walled structures [3]. This structure helps reduce the number of parts, shorten the overall assembly cycle of the structure, reduce the overall quality of the spacecraft, and improve the reliability of the aircraft performance and service life [4]. Therefore, the design and development of the part wall thickness tend to be thinner and the shape tends to be more complex, the requirements for the dimensional accuracy, shape error, and surface quality of the critical surface of the workpiece are higher [5]. However, on the one hand, titanium alloys have small deformation coefficients, low thermal conductivity, and low plasticity, resulting in poor relative cutting performance [6]. In the milling process, there are shortcomings such as large cutting force and short tool life, making it typical difficult-to-machine materials; On the other hand, thin-walled parts have poor process performance and low stiffness, and are very prone to deformation and vibration during processing [7, 8]. All of these restrict the further application of titanium alloy and therefore the manufacturing technology of titanium alloy curved thin-walled parts is a worldwide difficult problem. For the processing of titanium alloys, many scholars have studied it. Gürgen et al. [9] adopted a new multi-criteria decision-making (MCDM) method to study the different turning processes of Ti6Al4V alloy. This study was helpful to understand new non-traditional processing methods from the perspective of MCDM. Mehmet et al. [10] applied various soft computing methods to study different non-traditional turning operations. This method was helpful to understand the influence of various parameters in non-traditional machining methods and required less analysis time than finite element simulation. Wang, J et al. [11] presented an optimization algorithm to reduce the deformation of the workpiece, and the effectiveness of the algorithm was verified by experiments. Liu, C et al. [12] conducted experiments on jet-assisted milling of thin-walled titanium alloy parts, and the results showed that jet-assisted could improve cutting stability and reduce cutting force. Yi, J et al. [13] revealed the microscopic deformation mechanism of thin-wall milling by comparing the results of experiments and finite element values. Zha, J et al. [14] presented a milling method of thin-walled parts without auxiliary milling, which could ensure the machining accuracy and improve the machining efficiency by 40%. Sun C. al. [15] considered the stiffness characteristics of the tool and the workpiece, established a milling dynamics model, and verified the correctness of the model through experiments with different cutting depths.

However, the working conditions of titanium alloy thin-walled parts are very complicated, and it is necessary to find a stable processing method that can reduce the vibration of titanium alloy thin-walled parts. The composite processing technology obtained through the combination of traditional processing and special processing methods has become an important processing method for difficult-to-machine materials, complex thin-walled parts, and other parts [16, 17]. In

recent years, ultrasonic machining technology has been applied to some difficult-to-machine materials because of its excellent cutting characteristics for hard and brittle materials [18]. Ultrasonic composite machining can not only realize intermittent cutting, greatly reduce cutting force and cutting heat, enhance the stiffness of the processing system, and improve machining accuracy, but also suppress cutting chatter, improve machining quality, reduce tool wear, and reduce production costs [19]. Compared with high-speed milling, the effect of LTCUVM is not at the cost of increasing the spindle speed. Even at the conventional speed, it can still obtain higher machining accuracy and better surface quality, which requires a relatively low tool and machine tool spindle and greatly reduces the production cost. Many scholars apply ultrasonic machining to the milling of titanium alloy thin-walled parts. Jiang X. et al. [20] proposed an ultrasonic elliptical vibration milling method and proved that ultrasonic elliptical vibration milling has the outstanding characteristics of reducing cutting force, restraining tool offset, and improving cutting performance. Jiao. F et al. [21, 22] presented an ultrasonic vibration assisted (UVA) technology that made the workpiece vibrate along the feed direction, and clarified the cutting force and deformation characteristics in UVA milling. Experiments had shown that the radial cutting force of UVA milling was smaller than that of common milling (CM), and the thickness of the thin wall error would be affected by deflection displacement. Tong, J. et al. [23] developed the longitudinal-torsional composite ultrasonic vibration-assisted milling and designed experiments. The results showed that LTCUVM effectively reduced the average cutting force, the surface roughness, and the height of chatter marks. Zhang, M et al. [24] investigated a high-speed ultrasonic elliptical vibration milling method and conducted experiments. The results showed that compared to the common milling processing, the cutting force reduction and the relieving amount reduction were both about 20 to 30%, and the surface defects and roughness were also cut down. It can be seen from the above literature that the research on titanium alloy thin-walled parts mostly focuses on the milling force, the vibration displacement, and surface morphology of the workpiece, while the stiffness of thin-walled parts in the milling process is rarely studied. In addition, the shape of thin-walled parts studied is relatively simple, while in practical application, the thin-walled parts are mostly curved surfaces, such as the blades of aero engines.

In this paper, LTCUVM was used to improve the stiffness of titanium alloy thin-walled parts during the milling. The article was structured as follows: Section 2 analyzed the trajectory equation of cutting edge and the effect of stiffness enhancement in LTCUVM. Section 3 described the experimental devices and scheme. Section 4 detailed the analysis of the stiffness, with different curvatures, amplitudes, spindle speeds, feed speeds, and cutting depths, for titanium alloy thin-walled parts. Eventually, the conclusions were presented.

## 2 Theory

### 2.1 Trajectory equation of cutting edge

In the composite process of ultrasonic vibration and milling, the tool is used as the carrier of ultrasonic vibration, which can not only realize the processing of parts with different sizes and complex shapes but also make the ultrasonic vibration output more uniform and stable. In this article, the LTCUVM refers to a machining method that uses a tool as a vibration carrier.

In the milling of thin-walled parts, the cutting state of the tool and the vibration of the workpiece are important factors that affect the machining accuracy. Therefore, it is of great significance to study the cutting edge trajectory of LTCUVM. The milling model in LTCUVM was shown in Fig. 1.

In the milling process, a unit on the milling edge was taken to establish the milling edge path equation. In CM, the cutting edge path equation was as follows:

$$\begin{cases} x(t) = v_f \cdot t/60 + r \cdot \sin(2\pi nt/60) \\ y(t) = r \cdot \cos(2\pi nt/60) \\ z(t) = 0 \end{cases} \quad (1)$$

Where,  $v_f$  is the feed speed of milling cutter,  $r$  is the radius of milling cutter, and  $n$  is the spindle speed.

LTCUVM was based on the CM, which applied periodic vibration with the same frequency in the direction of tool axis and rotation. The cutting edge path equation of LTCUVM was as follows:

$$\begin{cases} x(t) = v_f \cdot t/60 + r \cdot \sin(2\pi nt/60 + B \cdot \cos(2\pi ft + \theta_2))/r \\ y(t) = r \cdot \cos(2\pi nt/60 + B \cdot \cos(2\pi ft + \theta_2))/r \\ z(t) = A \cdot \sin(2\pi ft + \theta_1) \end{cases} \quad (2)$$

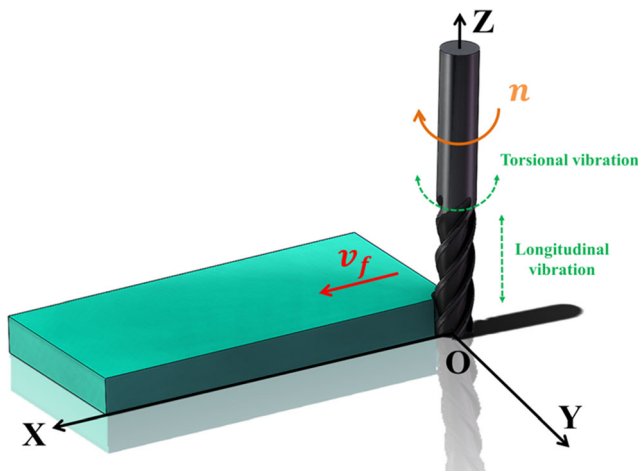


Fig. 1 Milling model in LTCUVM

Where,  $f$  is the ultrasonic vibration frequency,  $A$  is the amplitude of ultrasonic longitudinal vibration,  $B$  is the amplitude of ultrasonic torsional vibration,  $\theta_1$  is the initial phase of ultrasonic longitudinal vibration, and  $\theta_2$  is the initial phase of ultrasonic torsional vibration. The comparison of cutting edge trajectory between CM and LTCUVM was shown in Fig. 2.  $v_f = 300$  mm/s in Fig. 2 was to illustrate the torsional vibration phenomenon in LTCUVM more conveniently.

It can be seen from Fig. 2 that the trajectory of the cutting edge in LTCUVM had an obvious revolving phenomenon compared to CM. The cutting edge path of LTCUVM was projected to XOY plane to obtain Fig. 3.

It can be seen from Fig. 3 that the movement of the cutting edge of the milling cutter from point A to point D was a cycle. At point A, the ultrasonic torsion speed was equal to the spindle speed (but the tool had a tendency to reverse), and then the cutting edge moved from point A to point B. It could be seen that point A was the separation point between the tool and workpiece. When the cutting edge reached point B, the ultrasonic torsion speed was equal to the spindle speed again (but the tool tended to rotate forward), then the cutting edge moved from point B to point D. In the process of moving from point B to point D, the tool and workpiece would contact again, which was point C. If the feed rate was not taken into account, the point C and point A would coincide. Due to the effect of ultrasonic high-frequency vibration, the cutting edge and the workpiece were periodically separated and contacted. This movement can achieve the effect of reducing cutting heat and cutting force [25].

From the analysis in Fig. 3, the time taken for point C to point D was the effective cutting time. The effective cutting time was calculated as follows (Fig. 4):

Then, the value of  $T/t_l$  varies with torsion amplitude and spindle speed as shown in Fig. 5. It could be seen from Fig. 5 (a) that with the increase of ultrasonic torsional amplitude, the effective cutting time decreased, and the value of  $T/t_l$

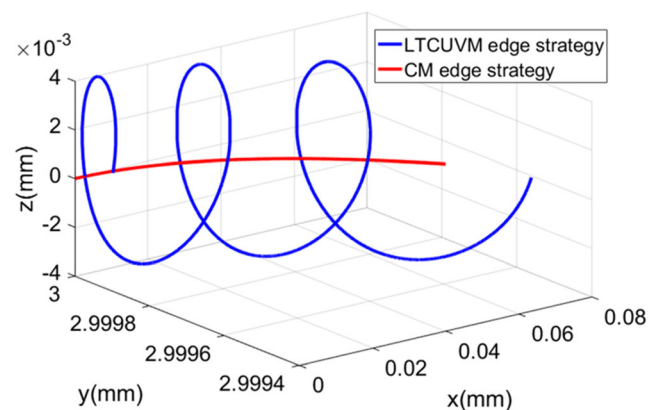


Fig. 2 Comparison of cutting edge trajectory between LTCUVM and CM. ( $r = 3$  mm,  $n = 1500$  r/min,  $v_f = 300$  mm/s,  $A = 0.004$  mm,  $B = 0.003$  mm,  $f = 33000$  Hz,  $\theta_1 = 0$ ,  $\theta_2 = 0$ )

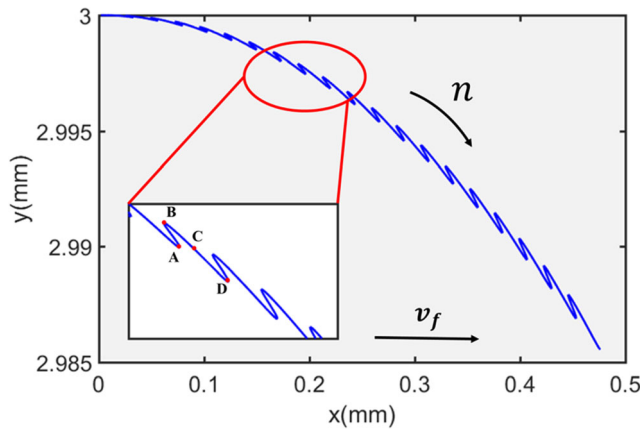


Fig. 3 Cutting edge trajectory of LTCUVM on XOY plane

increased. As shown in Fig. 5 (b), with the increase of spindle speed, the effective cutting time increased, and the value of  $T/t_l$  decreased.

### 2.2 Stiffness enhancement analysis of LTCUVM

As shown in Fig. 6, compared with ultrasonic longitudinal vibration, ultrasonic torsional vibration had more influence on the thickness direction of thin-walled parts. Then in LTCUVM, the high-frequency contact force of the thin-walled part in the direction of weak stiffness can be expressed as [26]:

$$F(t) = \begin{cases} F_0 & 0 \leq t \leq t_l \\ 0 & t_l < t \leq T \end{cases} \quad (3)$$

Where,  $F_0$  is the amplitude of contact force,  $t_l$  is the effective cutting time in one ultrasonic vibration cycle, and  $T$  is the ultrasonic vibration period of the milling cutter.

The high-frequency contact force  $F(t)$  was expanded according to Fourier series:

$$F(t) = \frac{t_l}{T} F_0 + \frac{2}{\pi} F_0 \sum_{n=1}^{\infty} \frac{1}{n} \left[ \sin\left(n \frac{t_l}{T} \pi\right) \cos(n\omega t) \right] \quad (4)$$

Then, the dynamic equation of thin-walled parts in the direction of weak stiffness could be expressed as follows:

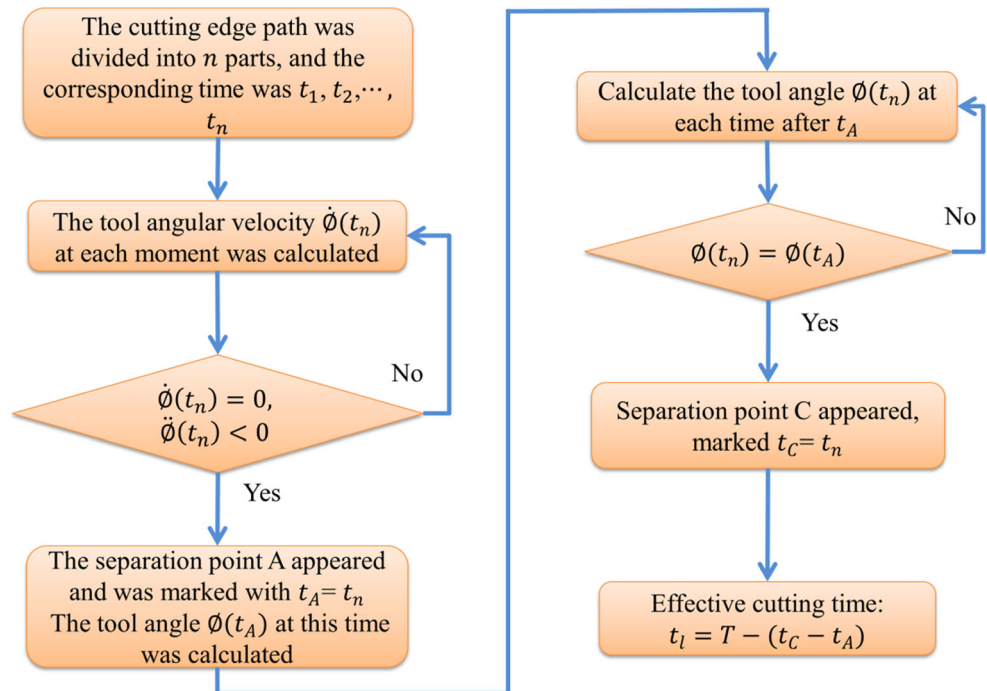
$$M\ddot{Y} + C\dot{Y} + KY = \frac{t_l}{T} F_0 + \frac{2}{\pi} F_0 \sum_{n=1}^{\infty} \frac{1}{n} \left[ \sin\left(n \frac{t_l}{T} \pi\right) \cos(n\omega t) \right] \quad (5)$$

Where,  $M$  is the mass matrix of thin-walled parts,  $Y$  is the deformation matrix in the thickness direction of thin-walled parts,  $C$  is the damping matrix of thin-walled parts,  $K$  is the stiffness matrix of thin-walled parts, and  $\omega$  is the circular frequency of ultrasonic vibration.

According to the above equation, the deformation of thin-walled parts in the direction of weak stiffness could be obtained as follows:

$$y = \frac{t_l F_0}{T k_y} + \sum_{n=1}^{\infty} \frac{\frac{F_0}{k_y} \cdot \frac{2}{n\pi} \sin\left(\frac{nt_l}{T} \pi\right)}{\sqrt{\left(1 - \frac{n^2 \omega^2}{\omega_n^2}\right)^2 + 4n\tau^2 \frac{\omega^2}{\omega_n^2}}} \sin(n\omega t + \varphi) \quad (6)$$

Fig. 4 Calculation flow chart of effective cutting time





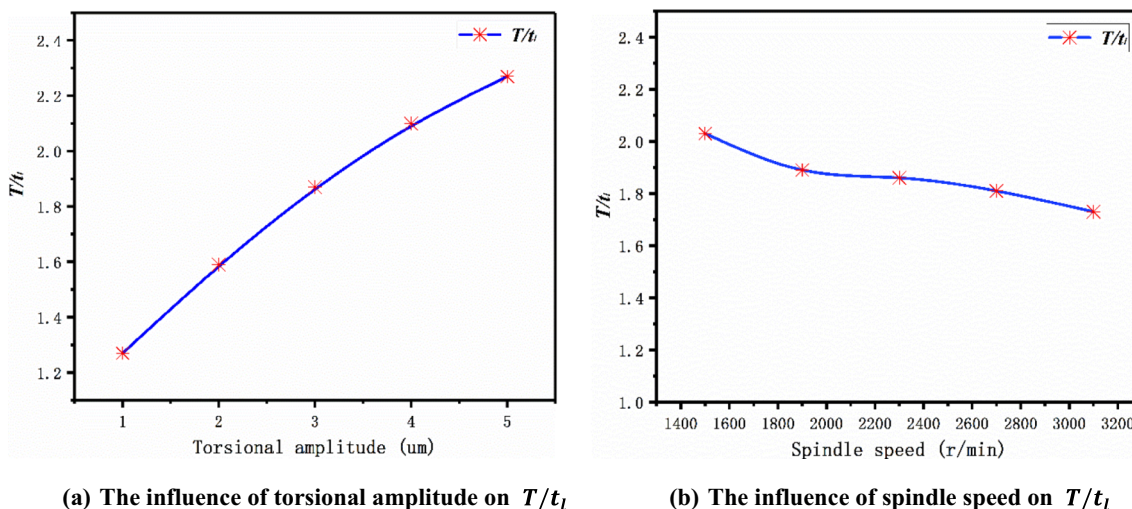


Fig. 5 The influence of torsional amplitude and spindle speed on  $T/t_l$  (a)The influence of torsional amplitude on  $T/t_l$ . (b)The influence of spindle speed on  $T/t_l$

Where,  $k_y$  is the structural stiffness of thin-walled parts,  $\omega_n$  is the natural circular frequency of the thin-walled parts,  $\tau$  is the damping ratio of thin-walled parts, and  $\varphi$  is the phase angle of contact force and displacement.

Then, Eq. (6) was modified as follows:

$$k_{ye} = \frac{k_y}{\frac{t_l}{T} + \frac{2}{\pi} \cdot \sum_{n=1}^{\infty} \frac{\frac{1}{n} \sin\left(\frac{nt_l}{T} \pi\right)}{\sqrt{\left(1 - \frac{n^2 \omega^2}{\omega_n^2}\right)^2 + 4n^2 \tau^2 \frac{\omega^2}{\omega_n^2}}} \sin(n\omega t + \varphi)} \tag{7}$$

Where,  $k_{ye}$  is the stiffness of thin-walled parts.

In LTCUVM,  $\omega \gg \omega_n$ , and then the series term in Eq. (7) would tend to zero. Therefore, Eq. (7) could be approximately

expressed as:

$$k_{ye} \approx \frac{T}{t_l} k_y \tag{8}$$

As shown in Eq. (8), the stiffness was inversely proportional to the effective cutting time ( $t_l$ ), and the stiffness ( $k_{ye}$ ) could be increased by  $T/t_l$  times compared with its structural stiffness. Further, the stiffness increased with the increase of ultrasonic torsional amplitude and decreased with the increase of spindle speed.

### 3 Experimental setup

#### 3.1 Acoustic system of LTCUVM

The system of LTCUVM employed in the test was composed of the ultrasonic generator, ultrasonic longitudinal-torsional composite horn, and wireless transmission system, as shown in Fig. 7.

The horn used in the experiment was a single excitation ultrasonic longitudinal-torsional composite horn with a spiral groove. When the longitudinal ultrasonic wave propagated in the horn and reached the spiral groove, the wave reflection and refraction would occur, and the longitudinal component and torsional component would be produced at the tooltip. The finite element software ANSYS was used to carry out modal analysis and modification. It could be seen from Fig. 8 that the vibration of the ultrasonic longitudinal-torsional horn at the flange was almost zero, the ultrasonic amplitude at the tooltip was the largest, and obvious longitudinal-torsional composite vibration was produced. In modal analysis, the resonant frequency is a very important modal parameter. It is considered that the connection between the horn, the transducer, and tool

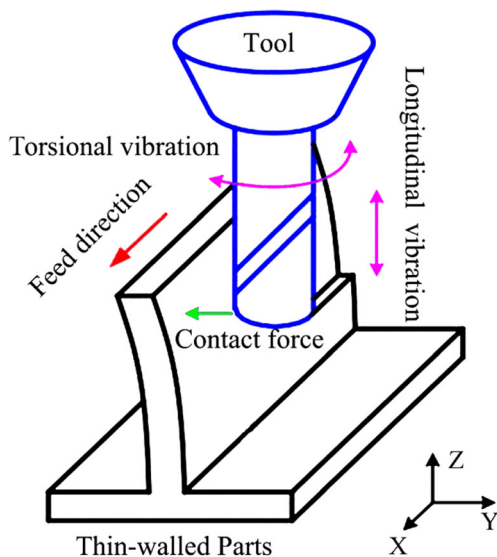
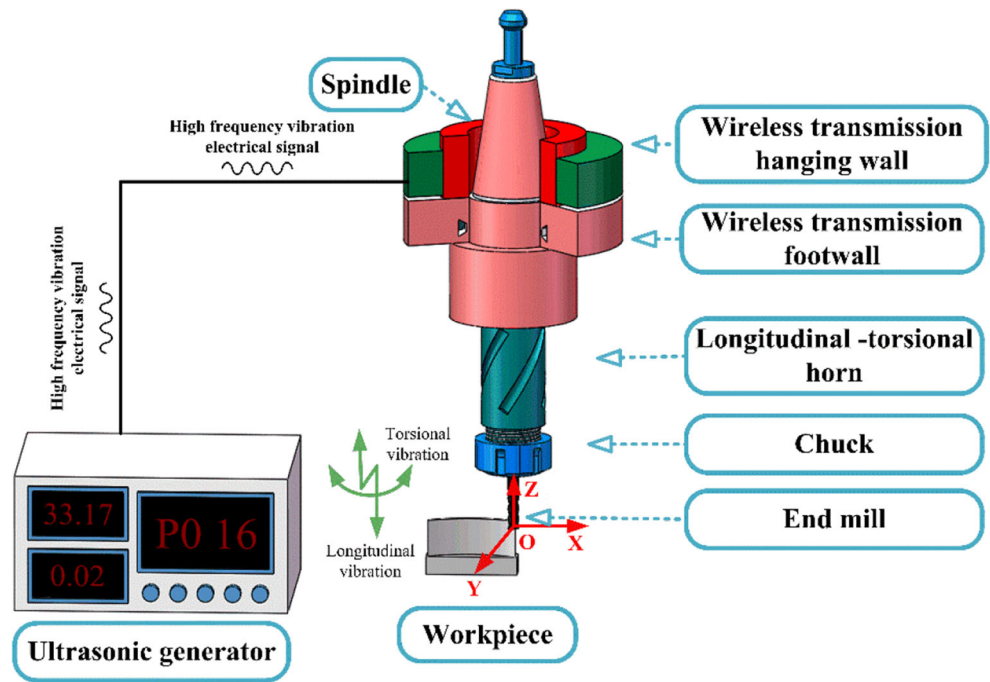


Fig. 6 Ultrasonic-assisted milling of thin-walled parts model

Fig. 7 System of LTCUVM



is ideal, and there is no energy loss in the theoretical design and simulation of the horn. However, it is inevitable to be affected by many factors during processing, which makes its performance change. Therefore, it is necessary to test the horn system. An impedance analyzer (PV70A) was used to test the resonant frequency of horn system (Table 1). The test results were shown in Fig. 9, and the resonant frequency was 33.15 KHz. Compared with the resonant frequency (30.875 KHz) obtained by modal analysis, the error was 6.8%, consequently, the design was feasible.

### 3.2 Description of experimental conditions

The machine tool employed in the test was a VMC850E vertical machining center. Figure 10 was the milling test platform of LTCUVM. The ultrasonic device was a self-developed

wireless transmission system and ultrasonic horn equipment. A cemented carbide end mill with a diameter of 3 mm, a blade length of 25 mm, and a total length of 75 mm was selected to mill titanium alloy thin-walled parts with different curvatures.

During the test, the Kistler system was used to collect cutting force, and the intelligent signal acquisition and processing analyzer (INV306DF) was used to collect vibration acceleration signals.

### 3.3 Experiment scheme

The chemical composition of titanium alloy used in the experiment was shown in Table 2. Titanium alloy curved thin-walled parts with a wall thickness of 1 mm, length of 50 mm, the height of 30 mm, and maximum curvature of  $K = 0$ ,  $K = 0.02$ ,  $K = 0.04$ , and  $K = 0.06$  were used in the test. To

Fig. 8 Modal analysis of LTCUVM

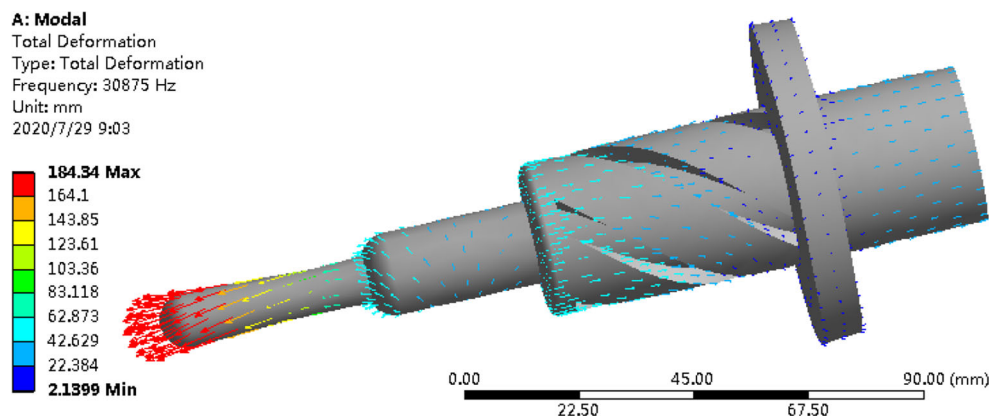


**Table 1** Material properties of ultrasonic longitudinal-torsional horn

Material	Density $\rho(\text{kg}/\text{m}^3)$	Yang’s model $E/(\text{GPa})$	Poisson’s ratio	Yield strength (MPa)
45# Steel	7800	210	0.28	355

study the stiffness characteristics of LTCUVM, curvature single factor test was designed, as shown in Table 3. According to the characteristics of the machine tool and previous tests [23], the appropriate processing parameters were selected, and the single factor test was designed, as shown in Table 4.

### 4 Test results and analysis

#### 4.1 The influence of curvature on stiffness

The experimental results were shown in Table 5. Both the milling force and the deformation of the thin-walled parts in LTCUVM were less than those in CM. Also, as can be seen from Fig. 11, the stiffness of thin-walled parts in LTCUVM was always greater than that in CM, no matter how the curvature changed. This was because the high frequency “cutting separation” state of LTCUVM reduced the average cutting force on the thin-walled parts, and then the deformation weakened; thus, the stiffness of thin-walled parts was improved. Moreover, the stiffness of LTCUVM and CM increased with the increase of curvature, which was because the structural stiffness of thin-walled parts also increased. It can also be seen from Fig. 11 that the enhancement multiples (compared with the stiffness of CM) of thin-walled parts increased first, then decreased and tended to be stable, and reached the maximum value when the curvature  $K = 0.02$ , the enhancement multiples were 2.23. The reason for this trend was when the curvature was less than a certain value, the structural stiffness of the thin-walled parts was small, and the ultrasonic strengthening effect on the thin-walled parts was obvious, then the curve showed an upward trend; while the curvature exceeded this value, the structural stiffness of the thin-walled parts was larger, and the strengthening effect of ultrasonic on the thin-

walled parts was weakened, then the curve showed a downward trend and tended to steady.

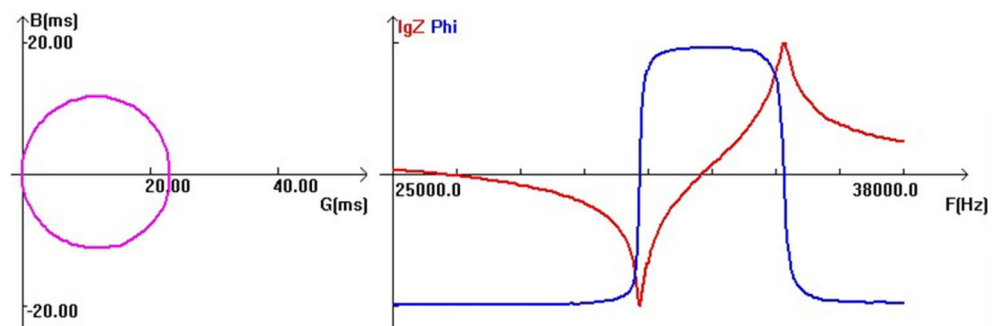
Besides, the surface vibration patterns of thin-walled parts under different curvature were observed by VHX-2000, and the results were shown in Fig. 12. Under different curvature, there was a lot of uneven vibration ripple, but the vibration ripple inclination had a great change. With the increase of curvature, the vibration ripple inclination gradually decreased, and the vibration ripple also gradually weakened. Under the same curvature, the surface chatter marks obtained by CM and LTCUVM were quite different; compared with CM, the surface chatter inclination of LTCUVM was relatively small. Similar chatter marks appeared on the surface of LTCUVM, and these chatter marks weakened with the increase of curvature. Compared with the CM, especially when the curvature  $K = 0.06$ , the chatter marks almost disappeared completely. This showed that under the same processing parameters, the larger curvature of thin-walled parts would improve its stiffness and reduce the deformation of the parts.

#### 4.2 Influence of milling parameters on stiffness

As shown in Fig. 13 (a), the stiffness of thin-walled parts in LTCUVM was always greater than that in CM. With the increase of ultrasonic amplitude, the stiffness had been increasing, and the maximum enhancement multiples could reach 3 times. This was because in a vibration cycle, with the increase of ultrasonic amplitude, the ultrasonic separation time increased, the corresponding effective cutting time decreased and then  $T/t_1$  increased. This was consistent with the analysis in 2.2. Therefore, the effective cutting time played a significant role in strengthening the stiffness of the system.

As given in Fig. 13 (b), with the increase of spindle speed, the stiffness of thin-walled parts in CM increased but decreased in LTCUVM, and the ultrasonic enhancement

**Fig. 9** Impedance analysis of horn system





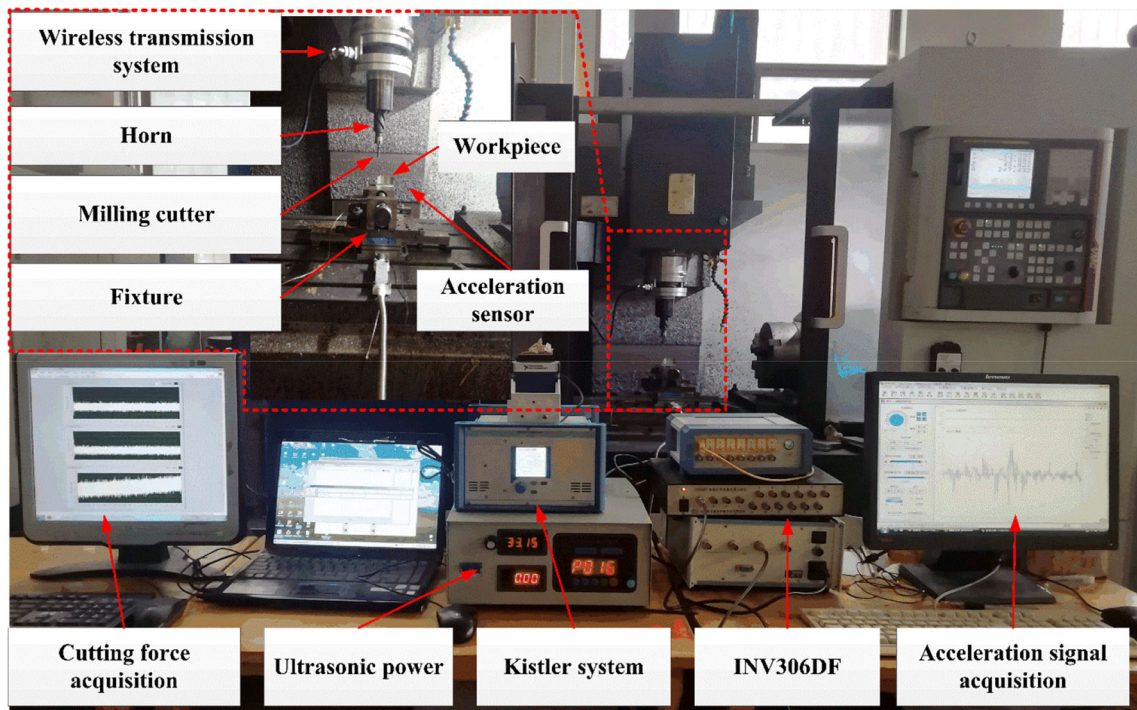


Fig. 10 Test platform of LTCUVM

multiples showed a downward trend. The reason for this phenomenon was that with the increase of spindle speed, the cutting force decreased, the deformation of thin-walled parts decreased, and the stiffness increased in CM. However, in LTCUVM, the effective cutting time increased, the effective cutting time increased, and then  $T/t_f$  decreased. Therefore, the enhancement multiples decreased gradually.

As illustrated in Fig. 13 (c) that with the increase of feed rate per tooth, the stiffness of thin-walled parts in CM and LTCUVM showed a downward trend, but the enhancement multiples were stable at about 2.3. This was because the material removal rate per unit time increased with the increase of

feed rate per tooth, the cutting force was gradually increasing, and the deformation was also increasing, but the increase was

Table 2 Chemical composition of titanium alloy

Element	Ti	Al	V	Fe	C	H	N	O
%wt.	90.348	5.820	3.710	0.016	0.016	0.004	0.010	0.002

Table 3 Single factor test of curvature

No	Maximum curvature	Spindle speed (r/min)	Feed per tooth (mm/z)	Ultrasonic amplitude (μm)
K1	0	2400	0.03	3
K2	0.02	2400	0.03	3
K3	0.04	2400	0.03	3
K4	0.06	2400	0.03	3

Table 4 Single factor test of processing parameters

No	Ultrasonic amplitude (μm)	Spindle speed (r/min)	Feed per tooth (mm/z)	Radial cutting depth(mm)	Curvature
A1	1	2400	0.03	0.3	0.02
A2	2	2400	0.03	0.3	0.02
A3	3	2400	0.03	0.3	0.02
A4	4	2400	0.03	0.3	0.02
A5	5	2400	0.03	0.3	0.02
S1	3	1500	0.03	0.3	0.02
S2	3	1900	0.03	0.3	0.02
S3	3	2300	0.03	0.3	0.02
S4	3	2700	0.03	0.3	0.02
S5	3	3100	0.03	0.3	0.02
F1	3	2400	0.01	0.3	0.02
F2	3	2400	0.03	0.3	0.02
F3	3	2400	0.05	0.3	0.02
F4	3	2400	0.07	0.3	0.02
F5	3	2400	0.09	0.3	0.02
C1	3	2400	0.03	0.1	0.02
C2	3	2400	0.03	0.25	0.02
C3	3	2400	0.03	0.4	0.02
C4	3	2400	0.03	0.55	0.02
C5	3	2400	0.03	0.7	0.02



**Table 5** Curvature single factor test results

No	CM			LTCUVM			Enhancement multiples
	Milling force	Deformation	Stiffness	Milling force	Deformation	Stiffness	
K1	74.75	2.61	28.64	50.5	1.08	46.75	1.63
K2	71.75	2.06	34.83	44.37	0.57	77.84	2.23
K3	69.62	1.64	42.45	38.25	0.49	78.06	1.83
K4	70.37	1.36	51.74	42.5	0.43	98.84	1.91

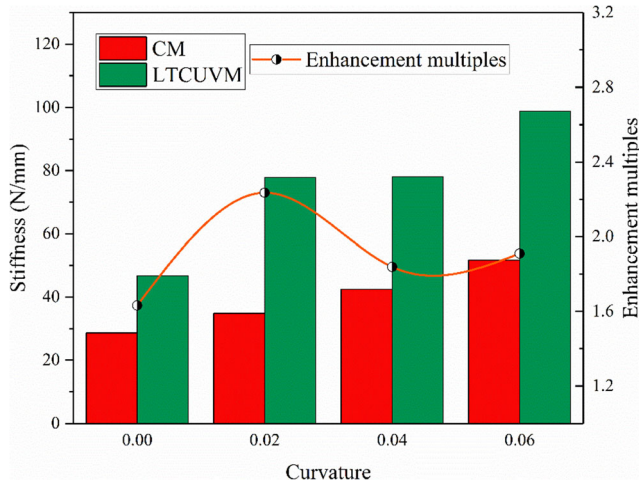
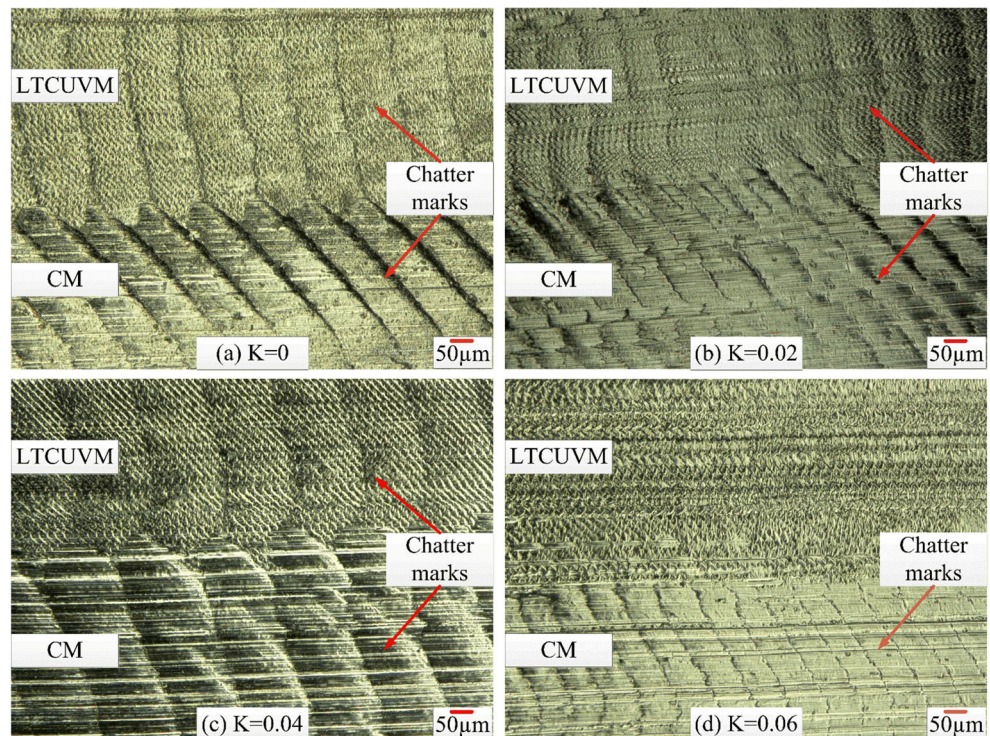


**Fig. 11** The effect of workpiece curvature on stiffness

the mainly tangential force, the increase of normal force was not very obvious, which led to a slight drop of stiffness. The increase of feed rate per tooth had no significant effect on the effective cutting time, for this reason, the enhancement multiples of ultrasonic stiffness were relatively stable.

As presented in Fig. 13 (d), with the increase of radial cutting depth, the stiffness of thin-walled parts in CM and LTCUVM showed a downward trend, and the enhancement multiples were about 2.3. This was because, with the increase of radial cutting depth, the normal force of thin-walled parts would increase, and the thin-walled parts were more prone to deformation, which made the stiffness of thin-walled parts decrease. However, the increase of radial cutting depth had little effect on the effective cutting time, the stiffness enhancement multiples thus only fluctuated in a small range.

**Fig. 12** Vibration marks under different curvatures. ( $v_f = 4.8$  mm/ $s, n = 2400$  r/min,  $A = 0.004$  mm,  $B = 0.003$  mm,  $f = 33000$  Hz)



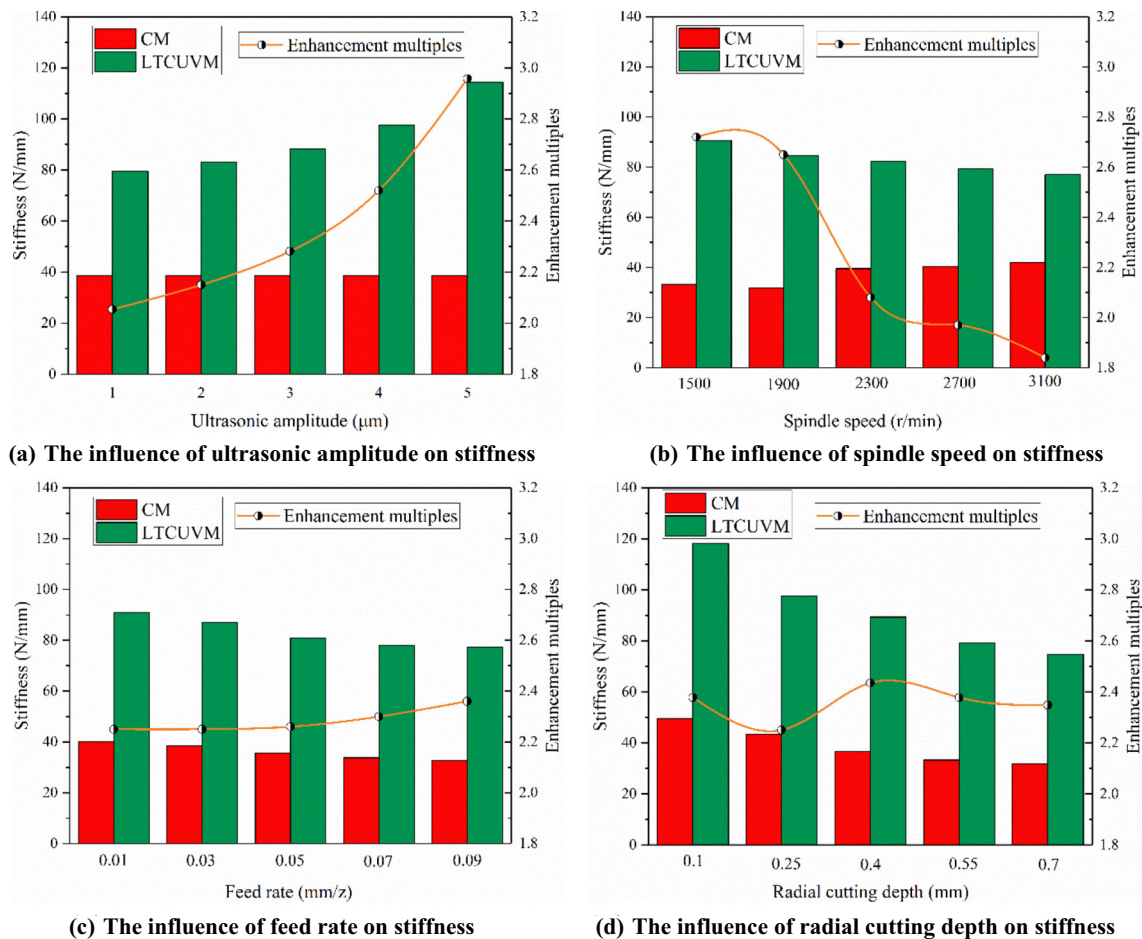


**Fig. 13** The influence of milling parameters on stiffness. (a) The influence of ultrasonic amplitude on stiffness. (b) The influence of spindle speed on stiffness. (c) The influence of feed rate on stiffness. (d) The influence of radial cutting depth on stiffness

## 5 Conclusions

The stiffness enhancement characteristics of titanium alloy curved thin-walled parts in LTCUVM were discussed in this paper. The specific conclusions were summarized as follows:

- (1) The cutting edge trajectory of LTCUVM was discussed. The continuous cutting of CM was transformed into intermittent cutting by LTCUVM. The torsional vibration of LTCUVM can improve the force and deformation of thin-walled parts in the direction of weak stiffness.
- (2) The stiffness of thin-walled parts was derived theoretically. In LTCUVM, the stiffness of the thin-walled parts can be increased by  $T/t_l$  times compared with its structural stiffness. In addition, with the increase of ultrasonic torsional amplitude, the effective cutting time decreased, and the value of  $T/t_l$  increased. With the increase of spindle speed, the effective cutting time increased, and the value of  $T/t_l$  decreased.
- (3) The experimental results showed that the stiffness of thin-walled parts in LTCUVM was always larger than

that in CM, but the enhancement multiples were different. With the increase of curvature, the stiffness enhancement multiples of thin-walled parts first increased and then decreased. In addition, the stiffness enhancement multiples of LTCUVM increased with increasing ultrasonic amplitude and decreased with increasing spindle speed. But with the increase of the feed per tooth and the radial depth of cut, it showed a stable state.

**Author contribution** Jinglin Tong contributed significantly to the analysis and manuscript. Penghui Zai performed the data analyses and wrote the manuscript. Peng Chen helped perform the analysis with constructive discussions. Ziqiang Liu contributed analysis tools. Zhiming Zhang put forward some important suggestions in the paper writing.

**Funding** This research was supported by the Henan Natural Science Foundation (162300410120).

**Data availability** Not applicable.

**Declarations**



**Ethics approval** This paper is new. Neither the entire paper nor any part of its content has been published or has been accepted elsewhere. It is not being submitted to any other journal as well.

**Consent to participate** Not applicable.

**Consent for publication** Not applicable.

**Conflict of interest** The authors declare no competing interests.

## References

- Chen P, Tong J, Zhao J, Zhang Z, Zhao B (2020) A study of the surface microstructure and tool wear of titanium alloys after ultrasonic longitudinal-torsional milling. *J Manuf Process* 53:1–11. <https://doi.org/10.1016/j.jmapro.2020.01.040>
- Zhao K, Zhang G, Ma G, Shen C, Wu D (2020) Microstructure and mechanical properties of titanium alloy / zirconia functionally graded materials prepared by laser additive manufacturing. *J Manuf Process* 56:616–622. <https://doi.org/10.1016/j.jmapro.2020.05.044>
- Bałon P, Rejman E, Świątoniowski A, Kiełbasa B, Smusz R, Szostak J, Cieślak J (2020) Thin-walled integral constructions in aircraft industry. *Procedia Eng* 47:498–504. <https://doi.org/10.1016/j.promfg.2020.04.153>
- Gajewski J, Golewski P, Sadowski T (2017) Geometry optimization of a thin-walled element for an air structure using hybrid system integrating artificial neural network and finite element method. *Compos Struct* 159:589–599. <https://doi.org/10.1016/j.compstruct.2016.10.007>
- Li Z, Tuysuz O, Zhu L, Altintas Y (2018) Surface form error prediction in five-axis flank milling of thin-walled parts. *Int J Mach Tool Manu* 128:21–32. <https://doi.org/10.1016/j.ijmachtools.2018.01.005>
- Al-Rubaie KS, Melotti S, Rabelo A, Paiva JM, Elbestawi MA, Veldhuis SC (2020) Machinability of SLM-produced Ti6Al4V titanium alloy parts. *J Manuf Process* 57:768–786. <https://doi.org/10.1016/j.jmapro.2020.07.035>
- Mamedov A, Lazoglu I (2016) Thermal analysis of micro milling titanium alloy Ti-6Al-4V. *J Mater Process Technol* 229:659–667. <https://doi.org/10.1016/j.jmatprotec.2015.10.019>
- Li Z, Zhu L (2019) Compensation of deformation errors in five-axis flank milling of thin-walled parts via tool path optimization. *Precis Eng* 55:77–87. <https://doi.org/10.1016/j.precisioneng.2018.08.010>
- Gürgen S, Çakır FH, Sofuoğlu MA, Orak S, Kuşhan MC, Li H (2019) Multi-criteria decision-making analysis of different non-traditional machining operations of Ti6Al4V. *Soft Comput* 23:5259–5272. <https://doi.org/10.1007/s00500-019-03959-8>
- Sofuoğlu MA, Çakır FH, Kuşhan MC, Orak S (2019) Optimization of different non-traditional turning processes using soft computing methods. *Soft Comput* 23:5213–5231. <https://doi.org/10.1007/s00500-018-3471-8>
- Wang J, Ibaraki S, Matsubara A (2017) A cutting sequence optimization algorithm to reduce the workpiece deformation in thin-wall machining. *Precis Eng* 50:506–514. <https://doi.org/10.1016/j.precisioneng.2017.07.006>
- Liu C, Sun J, Li Y, Li J (2018) Investigation on the milling performance of titanium alloy thin-walled part with air jet assistance. *Int J Adv Manuf Technol* 95:2865–2874. <https://doi.org/10.1007/s00170-017-1420-9>
- Yi J, Wang X, Jiao L, Li M, Xiang J, Yan P, Chen S (2018) Micro-flank milling forces considering stiffness of thin-walled parts. *Thin-Walled Struct* 95:2767–2782. <https://doi.org/10.1007/s00170-017-1249-2>
- Zha J, Liang J, Li Y, Zhang H, Chen Y (2020) Large cutting depth and layered milling of titanium alloy thin-walled parts. *Materials* 13. <https://doi.org/10.3390/ma13071499>
- Sun C, Shen X, Wang W (2016) Study on the milling stability of titanium alloy thin-walled parts considering the stiffness characteristics of tool and workpiece. *Procedia CIRP* 56:580–584. <https://doi.org/10.1016/j.procir.2016.10.114>
- Yang Z, Zhu L, Ni C, Ning J (2019) Investigation of surface topography formation mechanism based on abrasive-workpiece contact rate model in tangential ultrasonic vibration-assisted CBN grinding of ZrO<sub>2</sub> ceramics. *Int J Mech Sci* 155:66–82. <https://doi.org/10.1016/j.ijmecsci.2019.02.031>
- Xiang D, Wu B, Yao Y, Liu Z, Feng H (2019) Ultrasonic longitudinal-torsional vibration-assisted cutting of Nomex® honeycomb-core composites. *Int J Adv Manuf Technol* 100:1521–1530. <https://doi.org/10.1007/s00170-018-2810-3>
- Feucht F, Ketelaer J, Wolff A, Mori M, Fujishima M (2014) Latest machining technologies of hard-to-cut materials by ultrasonic machine tool. *Procedia CIRP* 14:148–152. <https://doi.org/10.1016/j.procir.2014.03.040>
- O Toole L, Kang C, Fang F (2020) Advances in rotary ultrasonic-assisted machining. *ISNM* 3:1–25. <https://doi.org/10.1007/s41871-019-00053-3>
- Jiang X, Liang H, Lu H, Dai J, Zhang D (2014) Investigation of ultrasonic elliptical vibration milling of thin-walled titanium alloy parts. *Acta Armamentarij* 35:1891–1897. <https://doi.org/10.3969/j.issn.1000-1093.2014.11.022>
- Jiao F, Yao C, Zhao L, Qi F (2018) Research on milling force in ultrasonic assisted end milling of titanium alloy thin-walled parts. *Key Eng Mater* 764:252–260. <https://doi.org/10.4028/www.scientific.net/KEM.764.252>
- Jiao F, Zhao L, Yao C, Qi F (2018) Research on milling deformation in ultrasonic vibration assisted end milling of titanium alloy thin-walled parts. *Key Eng Mater* 764:174–183. <https://doi.org/10.4028/www.scientific.net/KEM.764.174>
- Tong J, Wei G, Zhao L, Wang X, Ma J (2019) Surface microstructure of titanium alloy thin-walled parts at ultrasonic vibration-assisted milling. *Int J Adv Manuf Technol* 101:1007–1021. <https://doi.org/10.1007/s00170-018-3005-7>
- Zhang M, Zhang D, Liu J, Gao Z, Han X (2019) Mechanism and experiment of high-speed ultrasonic elliptical vibration milling of thin-walled titanium alloy parts. *J Univ Aeronaut Astronaut* 45:1606–1612. <https://doi.org/10.13700/j.bh.1001-5965.2018.0712>
- Ying N, Feng J, Bo Z (2020) A novel 3D finite element simulation method for longitudinal-torsional ultrasonic-assisted milling. *Int J Adv Manuf Technol* 106:385–400. <https://doi.org/10.1007/s00170-019-04636-8>
- JK (1985) The foundation and application of precision vibration cutting. Machinery Industry Press, Beijing

**Publisher's note** Springer Nature remains neutral with regard to jurisdictional claims in published maps and institutional affiliations.